

The evolution of the asymmetric disk structure of WZ Sge-type dwarf novae

Ryosuke Sazaki^{a,*} and Makoto Uemura^b

^a*Department of Physics, Graduate School of Advanced Science and Engineering, Hiroshima University, 1-3-1 Kagamiyama, Higashi-Hiroshima, Hiroshima 739-8526, Japan*

^b*Hiroshima Astrophysical Science Center, Hiroshima University, Kagamiyama 1-3-1, Higashi-Hiroshima, Hiroshima 739-8526, Japan*

E-mail: sazaki@astro.hiroshima-u.ac.jp

We report simultaneous optical and near-infrared photometry of the WZ Sge-type dwarf nova TCP J23580961+5502508 during its 2022 superoutburst, obtained with the 1.5-m Kanata telescope. Early superhumps were detected on three consecutive nights. The light-curve profiles were dominated by a single primary maximum on the first two days of our observation, whereas a distinct secondary minimum developed on the third day. Using the early superhump mapping technique, we reconstructed the accretion disk structure from the multi-band light curves. The resulting disk showed a prominent flaring structure on the leading side during the first two days. On the third day, an additional flaring region appeared on the trailing side, forming a two-armed pattern consistent with the structure predicted by the 2:1 resonance model. The disk morphology during the first two days suggests the presence of an additional mechanism operating in the earliest stage of early superhump development, prior to the establishment of the full 2:1 resonance geometry.

*87th Fujihara Seminar: The 50th Anniversary Workshop of the Disk Instability Model in Compact Binary Stars (DIM50TH2025)
22-26 September 2025
Tomakomai, Japan*

*Speaker

1. Introduction

Cataclysmic variables (CVs) are close binary systems consisting of a primary white dwarf and a secondary low-mass star that fills its Roche lobe (for a review, see [1]). In non-magnetic CVs, mass transferred from the secondary via Roche lobe overflow forms an accretion disk around the white dwarf. Dwarf novae (DNe) are a subclass of CVs that show recurrent outbursts with amplitudes of 2–8 mag and recurrence timescales ranging from days to years. These outbursts are widely interpreted in terms of the thermal–tidal instability model of the accretion disk (for a review, see [2]).

WZ Sge-type stars are a subclass of DNe characterized by extremely small binary mass ratios, $q \equiv M_{\text{secondary}}/M_{\text{WD}}$. They exhibit exceptionally long recurrence times (typically ~ 10 yr), as well as large outburst amplitudes (> 6 mag) and long outburst durations of order one month. A distinctive feature of WZ Sge-type systems is the presence of “early superhumps,” which appear as double-peaked modulations during the earliest phase of the superoutburst.

The period of early superhumps is nearly identical to the orbital period of the binary system [3]. Their amplitudes depend on the orbital inclination: while most early superhumps show amplitudes less than 0.05 mag, systems with high inclination can exhibit amplitudes exceeding 0.1 mag [4, 5]. Early superhumps also show reddening in color indices near the brightness maxima of the light curves [6] [7] [8]. These observational properties suggest that early superhumps originate from geometric effects, specifically the rotation of a non-axisymmetric flaring outer disk [5][9][10].

Theoretically, early superhumps are proposed to appear when the accretion disk expands to the 2:1 resonance radius, at which strong tidal torques from the secondary star act on the disk [9]. In contrast, ordinary superhumps, which are observed in SU UMa-type DNe, are associated with the 3:1 resonance that drives disk eccentricity, producing a precessing eccentric disk [11][12][13][14][15]. Because the 2:1 resonance can suppress the growth of the 3:1 resonance, ordinary superhumps appear only after the early superhump stage.

The 2:1 resonance scenario is currently the leading theoretical model for the origin of early superhumps. However, its validity remains uncertain due to the scarcity of observations obtained during the earliest stages of outbursts and the limited understanding of whether the model can reproduce the observed color variations. Uemura et al. (2012)[16] proposed a tomography technique, referred to as early superhump mapping, in which the vertical height distribution of the disk is reconstructed from multi-band light curves. Nevertheless, the number of studies applying this method remains small, and the diversity of disk structures has not been systematically examined. Moreover, although early superhumps are known to evolve in profile over time, no observational study has monitored these changes in multiple photometric bands from the very onset of an outburst. Consequently, the temporal evolution of the disk structure during the early superhump phase is still poorly understood.

An outburst of TCP J23580961+5502508 (hereafter TCP J2358) was discovered on 2022 September 30 by Tadashi Kojima¹. The autonomous observation system “Smart Kanata” detected the discovery report of TCP J2358 on the Transient Objects Confirmation Page (TOCP)², and

¹<http://www.cbat.eps.harvard.edu/unconf/followups/J23580961+5502508.html>

²<http://www.cbat.eps.harvard.edu/unconf/tocp.html>

follow-up observations were initiated immediately thereafter [17]. The likely quiescent counterpart of TCP J2358 is Gaia DR3 1993876650919517440, with $G = 20.6$ mag [18].

In this paper, we present simultaneous optical and infrared observations of TCP J2358 obtained during its 2022 outburst. These data enable, for the first time, an investigation of the temporal evolution of the disk structure over three consecutive nights, beginning prior to the outburst maximum.

The observational setup and data analysis procedures are described in Section 2, and the results are presented in Section 3. We discuss the implications of our findings in Section 4, and summarize our conclusions in Section 5.

2. Observation and Analysis

Time-resolved CCD photometric observations of TCP J2358 were conducted using the Hiroshima Optical and Near-InfraRed camera (HONIR), which enables simultaneous optical and near-infrared imaging [19]. HONIR is mounted at the Cassegrain focus of the 1.5-m Kanata telescope at the Higashi-Hiroshima Observatory. We used the V - and J -band filters, and the observations were performed in a dithering mode to facilitate accurate subtraction of the foreground sky.

3. Result

We conducted time-series photometry of TCP J2358 for three consecutive nights immediately after the discovery of the outburst, and successfully detected early superhumps. Figure 1 shows the phase-averaged light curves and color variation of the early superhumps in TCP J2358. The left, center, and right panels represent MJD 59852, 59853, and 59854, respectively. The overall trends of the light curves were removed by fitting and subtracting a quadratic function for MJD 59852 and linear functions for MJD 59853 and 59854. The detrended light curves were then folded using the early superhump period of $0.05940(1) \text{ d}^3$, and averaged into 0.05-phase bins.

The amplitude of the early superhump decreased from 0.16 mag on MJD 59852 to 0.10 mag on MJD 59853. As the outburst progressed, the secondary minimum became more pronounced. On MJD 59852, the early superhump profile was dominated by the primary maximum, especially in the V -band, whereas by MJD 59854 a clear secondary peak had developed in the folded light curve.

4. Discussion

We performed early superhump mapping following the method of Uemura et al. (2012)[16]. For this analysis, we used the phase-averaged light curves shown in Figure 1. We assumed that the orbital period P_{orb} is equal to the early superhump period, $P_{\text{ESH}} = 0.05940 \text{ d}$. The mass ratio q is not well constrained from our observational data. We therefore adopted $q = 0.078$, a representative value for WZ Sge-type DNe [4]. We confirmed that reasonable variations in q produce only minor changes in the reconstructed disk structure, including its radius, vertical height distribution, and the azimuthal location of the flaring region. TCP J2358 did not show eclipses and the amplitude of the early superhumps is relatively high. Thus, we adopt $i = 70^\circ$ for the mapping.

³<http://ooruri.kusastro.kyoto-u.ac.jp/mailarchive/vsnet-alert/26958>

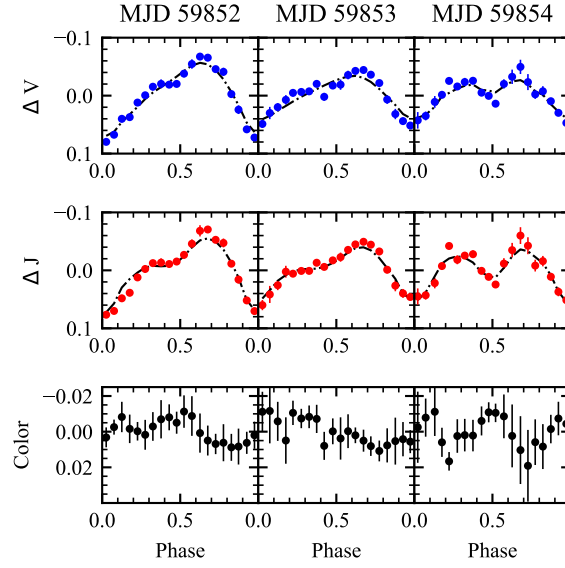


Figure 1: Phase-averaged light curves of the early superhumps of TCP J2358 from MJD 59852 to 59854. The top and middle panels show the V - and J -band light curves, respectively, and the bottom panels show the corresponding color variations. The left, center, and right columns correspond to MJD 59852, 59853, and 59854. Filled circles represent the observed light curves, while the dashed lines show the model light curves.

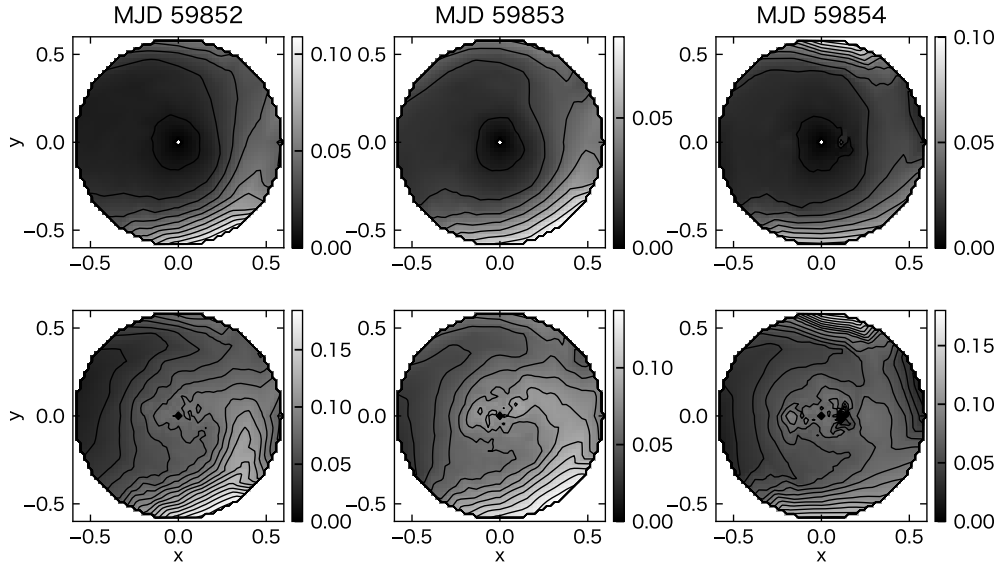


Figure 2: Reconstructed height maps of the accretion disk of TCP J2358 for the first three days of observation. The upper panels show the height h , and the lower panels show h/r , where r is the radial distance from the disk center. Both h , x , and y are normalized by the binary separation. Color scale and contour lines represent the same height distribution. The secondary star is located at $(x, y) = (1.0, 0.0)$ and orbits in the counterclockwise direction.

The reconstructed height maps of the accretion disk are shown in Figure 2. The upper panels display the height h of the disk normalized by the binary separation a , while the lower panels show the ratio h/r , where r is the radial distance from the disk center. The left, middle, and right panels correspond to the reconstructions for MJD 59852, 59853, and 59854, respectively. In these maps, the secondary star is located at $(x, y) = (1.0, 0.0)$, and it orbits counterclockwise.

Model light curves calculated from the reconstructed disks are shown as dashed lines in Figure 1. These models reproduce the overall behavior of the observed light curves, although the detailed local maxima and minima appear smoother. This smoothing arises because the reconstruction method imposes a smoothness constraint on the disk structure [16]. Reducing the smoothness constraint allows more complex disk structures to appear, but leads to overfitting and results in unphysically fine features. We therefore adopt the present smoothness setting as the optimal balance between fidelity to the data and physical plausibility.

In MJD 59852 and 59853, a flaring region is present only in the lower portion of Figure 2, corresponding to the leading side of the disk (i.e., the side facing the observer at orbital phase 0.0) near the outer edge. The structure is facing the observer at about orbital phase 0.75. On MJD 59854, an additional flaring region appears in the upper portion of the disk, corresponding to the trailing side. The highest points on the reconstructed height maps are located at $(x, y) = (+0.13, -0.58)$ with $h = 0.11$ on MJD 59852, $(+0.47, -0.36)$ with $h = 0.08$ on MJD 59853, and $(+0.13, +0.58)$ with $h = 0.10$ on MJD 59854. These values indicate that the maximum disk height remains at $h/a \sim 0.1$ during the first three days. This height is consistent with previous early superhump mapping studies [7, 16, 20]. Furthermore, the azimuthal extent of the flaring region gradually decreases with time.

In addition to the outer flaring regions, an arm-like structure extends inward from the lower (leading) side of the disk on MJD 59852 and 59853, and a similar feature may also be present on MJD 59854. We also note that the right side of each height map, corresponding to the region closer to the secondary star, is systematically more elevated than the opposite side on all three days.

The profile dominated by primary maximum in the light curves on MJD 59852 and 59853 corresponds to the presence of a single prominent flaring region in the disk. In contrast, the appearance of a clear double-peaked profile on MJD 59854 is associated with the development of two distinct flaring regions. Additionally, the systematically elevated right side of the disk contributes to the formation of the secondary minimum in the light curve, which remains shallower than the primary minimum.

In the reconstructed disks of other WZ Sge-type systems such as V455 And [16], OT J0120 [7], and PNV J00444033+4113068 [20], two flaring regions have been identified. However, our earliest two observations on MJD 59852 and 59853 suggest that the disk initially exhibits a single prominent flaring region. By MJD 59854, the reconstructed disk structure shows two flaring regions, consistent with the characteristic morphology reported in previous studies.

Osaki, Meyer (2002)[9] proposed that early superhumps are driven by the 2:1 resonance. This resonance is expected to generate a two-armed, spiral-shaped dissipation pattern in the accretion disk, and may exert a strong influence on angular momentum transport when the mass ratio is as large as $q = 0.1$ [21]. Consequently, the 2:1 resonance scenario predicts the presence of two flaring regions located at the outer edge of the disk. In our reconstruction, both flaring regions are clearly visible on MJD 59854 (Figure 2). In contrast, during MJD 59852 and 59853, the flaring structure on

the trailing side remains significantly weaker than that on the leading side. These results imply that, prior to the fully developed 2:1 resonance state, the disk may undergo an earlier phase that cannot be explained solely by the 2:1 resonance mechanism and instead requires an additional process to account for the observed asymmetry.

5. Summary

We performed simultaneous optical and near-infrared observations of the WZ Sge-type dwarf nova TCP J2358 during its 2022 outburst. The outburst showed clear early superhumps. Early superhumps were detected over three consecutive nights starting from the day of discovery. The early superhump profiles on MJD 59852 and 59853 were dominated by a single prominent maximum, while a distinct secondary maximum appeared on MJD 59854. The color variations of the early superhumps have a hint that is reddening around the hump maxima. Using the early superhump mapping method, we reconstructed the accretion disk structure from the multi-band light curves obtained over the three nights. The reconstructed disks on MJD 59852 and 59853 exhibited a flaring region on the leading side, while on MJD 59854, an additional flaring region appeared on the trailing side, consistent with the two-armed structure predicted by the 2:1 resonance model.

References

- [1] B. Warner, *Cataclysmic Variable Stars*, vol. 28 of *Cambridge Astrophysics Series*, Cambridge University Press, Cambridge (1995).
- [2] Y. Osaki, *Dwarf-Nova Outbursts*, *PASP* **108** (1996) 39.
- [3] R. Ishioka, M. Uemura, K. Matsumoto, H. Ohashi, T. Kato, G. Masi et al., *First detection of the growing humps at the rapidly rising stage of dwarf novae AL Com and WZ Sge*, *A&A* **381** (2002) L41 [[astro-ph/0111432](#)].
- [4] T. Kato, *WZ Sge-type dwarf novae*, *PASJ* **67** (2015) 108 [[1507.07659](#)].
- [5] T. Kato, *On the Origin of Early Superhumps in WZ Sge-Type Stars*, *PASJ* **54** (2002) L11 [[astro-ph/0201233](#)].
- [6] R. Matsui, M. Uemura, A. Arai, A. Sasada, T. Ohsugi, T. Yamashita et al., *Optical and Near-Infrared Photometric Observation during the Superoutburst of the WZ Sge-Type Dwarf Nova, V455 Andromedae*, *PASJ* **61** (2009) 1081 [[0908.4164](#)].
- [7] S. Nakagawa, R. Noguchi, E. Iino, K. Ogura, K. Matsumoto, A. Arai et al., *Multicolor Photometry of an Outburst of a New WZ Sge-Type Dwarf Nova, OT J012059.6+325545*, *PASJ* **65** (2013) 70 [[1304.1855](#)].
- [8] A. Imada, K. Isogai, T. Araki, S. Tanada, K. Yanagisawa and N. Kawai, *OAO/MITSuME photometry of dwarf novae. II. HV Virginis and OT J012059.6+325545*, *PASJ* **70** (2018) 2 [[1711.06080](#)].

- [9] Y. Osaki and F. Meyer, *Early humps in WZ Sge stars*, *A&A* **383** (2002) 574 [astro-ph/0112309].
- [10] H. Maehara, I. Hachisu and K. Nakajima, *Photometric Observation and Numerical Simulation of Early Superhumps in BC Ursae Majoris during the 2003 Superoutburst*, *PASJ* **59** (2007) 227 [astro-ph/0611519].
- [11] R. Whitehurst, *Numerical simulations of accretion discs - I. Superhumps : a tidal phenomenon of accretion discs.*, *MNRAS* **232** (1988) 35.
- [12] Y. Osaki, *A model for the superoutburst phenomenon of SU Ursae MAjoris stars.*, *PASJ* **41** (1989) 1005.
- [13] M. Hirose and Y. Osaki, *Hydrodynamic Simulations of Accretion Disks in Cataclysmic Variables: Superhump Phenomenon in SU UMa Stars*, *PASJ* **42** (1990) 135.
- [14] S.H. Lubow, *A Model for Tidally Driven Eccentric Instabilities in Fluid Disks*, *ApJ* **381** (1991) 259.
- [15] S.H. Lubow, *Simulations of Tidally Driven Eccentric Instabilities with Application to Superhumps*, *ApJ* **381** (1991) 268.
- [16] M. Uemura, T. Kato, T. Ohshima and H. Maehara, *Reconstruction of the Structure of Accretion Disks in Dwarf Novae from the Multi-Band Light Curves of Early Superhumps*, *PASJ* **64** (2012) 92 [1203.1358].
- [17] M. Uemura, Y. Koga, R. Sasaki, T. Yukino, T. Nakaoka, R. Imazawa et al., *Smart Kanata: A framework for autonomous decision-making in rapid follow-up observations of cataclysmic variables*, *PASJ* **77** (2025) 219 [2412.02092].
- [18] Gaia Collaboration, A. Vallenari, A.G.A. Brown, T. Prusti, J.H.J. de Bruijne, F. Arenou et al., *Gaia Data Release 3. Summary of the content and survey properties*, *A&A* **674** (2023) A1 [2208.00211].
- [19] H. Akitaya, Y. Moritani, T. Ui, T. Urano, Y. Ohashi, K.S. Kawabata et al., *Honir: an optical and near-infrared simultaneous imager, spectrograph, and polarimeter for the 1.5-m kanata telescope*, in *Ground-based and Airborne Instrumentation for Astronomy V*, vol. 9147, (Bellingham, WA), pp. 1520–1534, SPIE, SPIE, 2014.
- [20] Y. Tampo, K. Isogai, N. Kojiguchi, M. Uemura, T. Kato, T. Tordai et al., *PNV J00444033+4113068: Early superhumps with 0.7 mag amplitude and non-red color*, *PASJ* **74** (2022) 1287 [2208.04251].
- [21] D.N.C. Lin and J. Papaloizou, *Tidal torques on accretion discs in binary systems with extreme mass ratios.*, *MNRAS* **186** (1979) 799.